Phenomenology of Rayleigh-Taylor Turbulence

If a heavy fluid lies above a light one, the gravity-driven Rayleigh-Taylor (RT) instability develops. At later stages, this unstable flow becomes turbulent. The most striking feature of RT turbulence is the formation of a turbulent mixing zone of width L that grows quadratically with time:

$$L \approx \alpha \mathcal{A} g t^2 \,. \tag{1}$$

Here, $\mathcal{A}$ is the Atwood number, related to the fluid densities $\rho_{1,2}$ by $\mathcal{A} \equiv (\rho_1 - \rho_2)/(\rho_1 + \rho_2)$, and g is the acceleration of gravity. The law (1) was observed in many numerical and laboratory experiments. Numerical and experimental values of the dimensionless coefficient α in Eq. (1) vary from 0.02 to 0.07.

Recently we proposed a phenomenological theory explaining the hierarchy of scales and the spectra of velocity and density fluctuations in a specific regime of $3d$ RT turbulence: for low $\mathcal{A}$ (i.e., in the Boussinesq approximation) and for miscible fluids [1]. The theory is based on the law (1) and also on a common feature of multi-scale organization in hydrodynamic turbulence, viz., that small scales adjust adiabatically to changes in large scale characteristics. The phenomenology predicts that, in the wide range of scales between the integral scale, L, and the viscous scale, η, energy cascades down scale (as observed numerically and experimentally) and the Kolmogorov estimate for the velocity increment (difference),

$$\delta v_r \sim (\epsilon r)^{1/3} \,, \tag{2}$$

holds. Here ϵ is the energy flux per unit mass, $\epsilon \sim \mathcal{A}^2 g^2 t$, which grows linearly with time. It was shown in Ref. [1] that the Kolmogorov scenario is self-consistent, in the sense that even though the RT turbulence is buoyancy driven at scales $\sim L$, the effect of buoyancy on turbulence becomes irrelevant at smaller scales, $r \ll L$. This self-consistent logic is an adaptation (to the RT turbulence setting) of the Shraiman-Siggia arguments, introduced in the context of Boussinesq convection. The phenomenology also predicts that the viscous scale η decreases with time as

$$\eta \sim \left(\frac{\nu^3}{\mathcal{A}^2 g^2 t} \right)^{1/4} \,, \tag{3}$$

where ν is the kinematic viscosity. Comparing Eq. (1) and Eq. (3) one finds that the turbulent description is self-consistent, i.e., $L \gg \eta$, for $t \gg \nu^{1/3} \mathcal{A}^{-2/3} g^{-2/3}$.

It is clear that the adiabatic and Kolmogorov-like arguments leading to the estimate (2) are not restricted to the miscible case considered in Ref. [1]. In particular, the general argument suggests that the Kolmogorov picture also holds within some range of scales for the immiscible case. In this case, however, surface tension should play an essential role in the mixing zone. Thus the problem addressed in the recent paper [2] was to identify and study phenomena related to surface tension.

We examined in [2] the dynamics of two immiscible fluids when the heavier fluid is placed initially above the lighter one. This configuration leads to RT instability, which eventually develops into RT turbulence. The size of the turbulent mixing zone (and thus the amount of fluid entrained in the turbulent motion) grows according to Eq. (1). Hydrodynamic motion at scales $\sim L$ is driven by buoyancy. At smaller scales the direct (i.e., directed towards smaller scales) cascade of (kinetic) energy is realized, leading to the estimate (2). The cascade is accompanied by mutual penetration of the fluids, which is initiated by the injection of pure fluid jets into the mixing zone. The collision of jets of different fluids produces complex (fractal) interfacial structures. Drops of both types are permanently shed from the interface; the result is the creation of an emulsion-like state. A schematic view of a snapshot taken inside the mixing zone, illustrating the density distribution, is shown in Fig. 1. Notice that the exact shapes of the drops are by no means fixed, as fluctuations in the local radius of curvature of the interface are of the order l, i.e., the typical drop size. Surface tension does not allow drops to have size much smaller than l.

If the typical drop size is larger than the viscous scale, $l \gg \eta$, then l can be estimated to be the scale where the kinetic energy density of the fluids, $\varrho(\delta v_l)^2$, and the interfacial energy density, σ/l, are of the same order:

$$l \sim \left(\frac{\sigma^3}{\mathcal{A}^4 \varrho^3 g^4 t^2} \right)^{1/5} \,, \tag{4}$$

where ϱ is the mean mass density, $\varrho = (\rho_1 + \rho_2)/2$, and σ is the surface tension coefficient. According to Eq. (4), the characteristic drop size l decreases with time t, generating an emulsion that is progressively more dispersed. Dynamically, the permanent decrease in the typical drop size is realized through creation (shedding) of new drops as well as through breakup of already existing drops into smaller ones. The estimate (4) is correct provided that the scale l is much smaller than L; this requirement corresponds to the condition

$$t \gg \left(\frac{\sigma}{\mathcal{A}^3 \varrho g^3} \right)^{1/4} \,. \tag{5}$$

This inequality emphasizes that at large scales, $\sim L$, gravity overcomes surface tension (which tends to

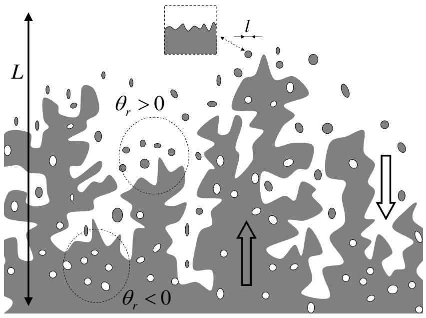

Figure 1: Schematic view of the mass distribution snapshot. Different mass densities are marked as grey/light and white/heavy, respectively. Circular domains bounded by dashed lines correspond to regions dominated by heavy and light (fluids. Density distribution within any of the domains is not homogeneous: drop-rich (emulsion) regions alternate with drop-free regions. Arrows indicate mean direction of the flow in the corresponding regions. Drops are shed from single-phase tongues possessing fractal shape. The inset on the top of the Figure illustrates that surfaces of the drops are populated by capillary waves.

stabilize the RT instability). Another condition, $l \gg \eta$, results in

$$t \ll t_0, \quad t_0 = \frac{\sigma^4}{\mathcal{A}^2 \varrho^4 g^2 \nu^5} \,. \tag{6}$$

This inequality means that the Kolmogorov cascade is insensitive to viscosity at scales $\sim l$. We assume that the inequalities (5) and (6) are compatible, thus leading to the condition $\sigma^3 \gg \mathcal{A}\varrho^3 g \nu^4$.

If $t \ll t_0$, the drop size, l, lies in between the integral scale, L, and the viscous scale, η. In the range of scales bounded from above by L and from below by l, the Kolmogorov in-volume cascade is realized. One finds that at smaller scales, $r < l$, turbulence inside and outside drops is also of the Kolmogorov type. As far as dynamics on the interface (surfaces of the drops) is concerned, we claim that a turbulent cascade of capillary waves takes place. The capillary wave dynamics opens an additional channel for energy transfer to small scales. The energy flux, coming from the integral scale L, splits in two parts at the scale l: a part of the energy cascades further (towards η) in the bulk (the mechanism being equivalent to that for single-phase turbulence) while the remainder (which is roughly of the same order as the volume part) feeds capillary fluctuations, giving rise to the capillary wave energy cascade at the surfaces of drops.

Capillary waves are excited at the scale l by the inertial motion; then capillary wave interactions lead to the formation of a cascade. The cascade is of a weak turbulence kind, i.e., the roughness (degree of non-flatness) of the interface decreases with scale. Therefore, zoomed at the scale $r \ll l$, the interface can be viewed as an almost flat one populated by capillary waves. Such zoomed portion of the interface is shown schematically as an inset in Figure 1. The fluctuation spectra for the capillary wave cascade were derived by Zakharov and co-workers. Using their results, one finds that the pair correlation function of the wave-generated velocity field, measured at two points on the interface lying distance r apart from each other, is

$$\langle \boldsymbol{v}(\boldsymbol{R})\boldsymbol{v}(\boldsymbol{R}+\boldsymbol{r})\rangle \sim (\epsilon l)^{2/3}(l/r)^{1/4} \,. \tag{7}$$

The typical surface elevation between the two points is estimated as $h_r \sim r(r/l)^{3/8}$. Therefore, the typical slope, h_r/r, characterizing an effective nonlinearity of the problem, decreases with the scale. This estimate confirms that the wave turbulence at the interface is weak. It is also straightforward to check that the nonlinear interaction time at the scale r within the wave turbulence range decreases with scale, $\propto r^{3/4}$, thus making our adiabatic description well justified. We also find that velocity fluctuations induced by the capillary waves (7) are stronger than respective fluctuations in the bulk. Therefore, the interface turbulence is insensitive to fluctuations in the bulk. On the other hand, velocity fluctuations at a scale r generated by surface waves become negligible beyond distance r from the interface. This explains why turbulent fluctuations in the bulk are insensitive to fluctuations at the interface. The capillary waves are dissipated at the scale $r_0 = \varrho\nu^2/\sigma$. One concludes that the capillary wave interval, bounded by l from above, by r_0 from below and containing η scale in between, shrinks with time, so that the three scales become comparable at t_0. Later on, for $t \gg t_0$, the characteristic drop size l becomes smaller than η, which, in turn, becomes smaller than r_0. Therefore, the capillary cascade is absent at this stage. The scale l emerges now as the result of a balance between the capillary force: $l \sim \sigma(\mathcal{A}\varrho g\sqrt{\nu t})^{-1}$, which guarantees that the capillary scale decreases with time faster than the viscous scale.

References

[1] M. Chertkov, *Phenomenology of Rayleigh-Taylor Turbulence*, Phys. Rev. Lett. **91**, 115001 (2003).

[2] M. Chertkov, I. Kolokolov and V. Lebedev, *Effects of surface tension on immiscible Rayleigh-Taylor turbulence*, submitted to Phys. Rev. Lett. 09/2004.

Contact Information: Michael Chertkov – Complex systems Group and Center for Nonlinear Studies, Theoretical Division, Los Alamos National Laboratory, MS-B258, Los Alamos, NM, 87545, Phone: (505) 665-8119, email: chertkov@lanl.gov.